Influence of Progressive vs. Minimal Canal Preparations on the Fracture Resistance of Mandibular Molars: A Finite Element Analysis

Michael Smoljan
Marquette University

INFLUENCE OF PROGRESSIVE VS. MINIMAL CANAL PREPARATIONS ON THE FRACTURE RESISTANCE OF MANDIBULAR MOLARS: A FINITE ELEMENT ANALYSIS

by

Michael J. Smoljan, D.D.S.

A Thesis Submitted to the Faculty of the Graduate School,
Marquette University,
in Partial Fulfillment of the Requirements for
the Degree of Master of Endodontics

Milwaukee, Wisconsin

May 2020

ABSTRACT
INFLUENCE OF CANAL PREPARATION WITH PROGRESSIVELY VS. MINIMALLY TAPERED INSTRUMENTS ON THE FRACTURE RESISTANCE OF MANDIBULAR MOLARS: A FINITE ELEMENT ANALYSIS

Michael J. Smoljan, D.D.S

Marquette University, 2020

INTRODUCTION: Several file systems have been recently introduced with the objective of preserving coronal dentin. There is limited research comparing the role of canal shaping on preservation of pericervical dentin and its role in fracture resistance. The aim of this study is to investigate the effect of minimal canal taper on residual tooth strength and stress distribution after root canal treatment.

METHODS: Two pre-accessed mandibular molar TruTeeth (Acadental Endo 3DP, Lenexa, KS) were subject to simulated endodontic treatment in this study. One tooth was instrumented with ProTaper Gold (Dentsply, Tulsa, OK) to F2 (25/0.08v progressive taper) in the mesial canals and F3 (30/0.09v progressive taper) in distal canals using manufacturer protocol. The other tooth was instrumented with V-Taper 2H (SSWhite Dental, Lakewood, NJ) to 25/0.06v (minimal taper) in mesial canals and 30/0.06v (minimal taper) in the distal canals. The two teeth were scanned using microcomputed tomography (micro-CT,) and STL (stereolithography) surface meshes were developed for Finite Element Analysis (FEA). Four models were evaluated assessing the type of instrumentation and presence of resin access filling. The results of the FEA provided quantitative and qualitative measurements for Von Mises (VM) stress distribution and total deformation.

RESULTS: Under a 200-N multipoint load, the maximum VM stress was greater in the Pro-Taper Gold prepared models than in the V-Taper 2H prepared models. The models without an access restoration had higher total deformation values than the models with a resin filled access. In all models, total deformation values were highest in the clinical crown on the buccal aspect of the tooth. The greatest stress values were found in the pericervical dentin, and stresses decreased apically through the root.

CONCLUSIONS: Within the limitations of this study, it can be concluded that the maximum stress values within the tooth prepared by ProTaper Gold were higher than those in the tooth prepared by V-Taper 2H. The minimally invasive instrumentation of the V-Taper 2H system preserves more pericervical dentin which may increase the resistance to fracture.

ACKNOWLEDGEMENTS

Michael J. Smoljan, D.D.S.

I would like to thank Marquette University School of Dentistry and the endodontic department for giving me the opportunity become an endodontist.

I would like to acknowledge the members of my thesis committee without whom this thesis would not be possible: Dr. Mohamed Ibrahim, Dr. Arndt Guentsch, and Dr. Joe Gaffney.

Dr. Ibrahim, thank you for helping me pursue this idea. Thank you for the support, encouragement, and guidance to overcome the obstacles that were faced in completing this project.

I would also like to thank Dr. Mostafa Hussein, Dr. Lance Hashimoto, Dr. Brian Ong, Dr. John Moore, Dr. Elizabeth Chybowski, Dr. Joseph DeGuzman, Dr. Gordon Barkley, Dr. Jon Irelan, and Dr. Alex Moore for their roles in this project and in my endodontic training. I'll forever be grateful for the mentorship from the Marquette faculty.

I want to thank my co-residents Drs. Abby Yavorek, Hunter Housley, Max Montatskiy, Timothy Gainey, Igor Sulim, Enida Haxhia, Lauren Loney, and Tom Korte for your friendship. I've learned the most from all of you and am so grateful that our path's crossed at Marquette.

Finally, I would like to thank my wife, Annie, and the rest of my family. I would not be where I am today without their sacrifices, love, and support.

TABLE OF CONTENTS

List of Tables

LIST OF FIGURES

INTRODUCTION

Non-surgical root canal therapy includes the chemo-mechanical preparation of the root canal system with subsequent filling in three dimensions to eliminate the root system as a source of infection or inflammation to the apical periodontium. Root canal instrumentation should debride the canal of pulp tissue, remove microbes, remove affected dentin, and prepare the canal from obturation (1). Chemo-mechanical preparation of the root canal is known to be the most important phase in root canal preparation. As the root canal system is enlarged with mechanical instrumentation, the bacterial load and associated debris harboring bacteria are significantly reduced (2). Further evidence confirmed the role of instrumentation in reducing the microbial load but emphasized the role of chemical disinfection to achieve the lowest bacterial loads possible (3).

For over 30 years, endodontists have been using rotary instruments to prepare root canal systems. Modern advancements in endodontics such as the dental operating microscope, ultrasonic instruments, heat treated nickel-titanium (NiTi) files, and supplemental irrigating systems have contributed to the shift towards minimally invasive endodontics (4). This paradigm shift focuses on the modifiable treatment techniques by the operator to preserve tooth structure while still accomplishing the goals of endodontic treatment. Much of this focus centers on endodontic access and instrumentation which is directly related to the remaining tooth structure present after root canal preparation. It has been proposed that the most valuable tooth structure to be preserved is pericervical dentin (PCD). PCD refers to the dentin located 4 mm coronal and 4 mm apical to crestal bone and is believed to play a crucial role in transferring occlusal forces through the root

(5). Preventing unnecessary removal of tooth structure may help reduce the incidence of vertical root fractures and propagation of cracks, both of which are causes of failure in endodontically treated teeth (4).

There have been countless file systems introduced to the market with different tapers, cross section, and heat treatments to maximize the files' clinical efficiency. Progressively tapered file systems such as the ProTaper Gold System (Dentsply Tulsa Dental Specialties, Tulsa, OK) and others use variable tapered instrument sequences or single files to create a deep shape that facilitates adequate irrigation of the canal at the apex. Minimally tapered files such as the V-Taper 2H (SSWhite Dental, Lakewood, NJ), and others have been developed to have a maximum flute diameter of 0.7 to 0.8 mm that preserves PCD while simultaneously allowing irrigant to reach the apical one third of the canal. There is limited research comparing the role of canal shaping on preservation of pericervical dentin and its role in fracture resistance. The aim of this study is to investigate the effect of minimal canal taper on residual tooth strength and stress distribution after root canal treatment using finite element analysis (FEA).

LITERATURE REVIEW

Goal of Endodontic Treatment

The goal of endodontic treatment is to prevent or treat apical periodontitis (6). Apical periodontitis occurs when bacteria invade the dental pulp and root canal system (7,8). Endodontic infection progresses as the bacteria occupies the root canal space and the bacteria form biofilms that become increasingly more difficult to remove (9). Root canal therapy (RCT) is a common dental procedure performed to remove or reduce biofilm within the canal space and treat odontogenic infections. Treatment is composed of access, cleaning and shaping with chemo-mechanical disinfection, and sealing of the root canal system to prevent reinfection (10). Proper disinfection is critical to the success of RCT as evidence suggests that residual biofilm is most common cause of endodontic failure (11).

Endodontic Instrumentation

Mechanical preparation via manual and rotary instrumentation is intended to remove tissue, infected tooth structure, debris, and bacteria from the root canal system. If the appropriate amount of tissue, debris, and bacterial contents are not removed from the root canal system, positive outcomes are far less likely (1). The aim of modern instrumentation techniques involves enlarging the apical third of the root canal to allow for proper debridement, disinfection, and sealing of the canal space while maintaining the original root canal anatomy. The degree of shaping is determined by the preoperative root dimension, the obturation technique, and the restorative treatment plan. The apical constriction is believed to be the narrowest part of the root canal. The apical constriction is not typically round and is often ovoid or irregular in shape (12). Histological studies evaluating the morphology of root apices suggest that the apical constriction is 300 to 350 microns (13,14). These findings suggest that based on a biological approach to instrumentation the minimum apical preparation of a canal should be to ISO size 30 (15). Conversely, studies have also shown that smaller apical sizes can facilitate adequate disinfection (16,17). Regardless of the apical size of the preparation, it is not possible to sterilize the root canal system (18).

Modern advancements in techniques, obturation materials, and irrigation protocols allow for more conservative approaches in endodontic instrumentation. There have been a variety of instruments and technique advancements that can achieve the objectives of instrumentation (10). Currently, there are more than fifty canal preparation systems that vary in terms of taper, cross-section, and material. The special designs of orifice shapers and glide path files have changed the way that clinicians instrument and recent techniques such as minimally invasive endodontics have emerged.

The term minimally invasive endodontics has been used to describe smaller apical shapes and minimal instrumentation techniques to conserve dentin throughout the root (4). One of the first files on the market that focused on minimal instrumentation was the TRUshape system (Dentsply, Tulsa, OK) that had a maximum flute diameter of 0.75 mm (19). Advancements in rotary instrumentations have led to improvements in the ability to shape root canals while simultaneously reducing the amount of procedural complications (20).

ProTaper Gold

The ProTaper Gold (Dentsply, Tulsa, OK) rotary system consisting of shaping (S1, S2) and finishing (F1, F2, F3, F4, F5) instruments, along with an orifice shaping instrument (SX), is made of a proprietary metallurgy that increases it flexibility and resistance to fatigue (21). The S1 and S2 instruments have D_0 diameters of 0.17 mm and 0.20 mm with a maximal flute diameter 1.20 mm. The shaping instruments have multiple increasing percentage tapers over the length of their cutting blades. The progressively tapered file design allows each instrument to contact a specific area of the canal in a "crown down" fashion, focusing on the middle and coronal thirds of the root canal space. The finishing instruments possess decreasing tapers along their lengths and cut in the apical third of the canal (22). The F1, F2, F3, F4 and F5 instruments have D_0 diameters of 0.20, 0.25, 0.30, 0.40 and 0.50 mm, respectively. The F1, F2, and F3 files have maximum flute diameters of 1.13, 1.22, and 1.26 mm, respectively (23). The F4 and F5 are files used for very large canals and the taper profile of these files is not published.

V-Taper 2H

V-Taper 2H (SS-White Dental) is the second-generation system made with controlled memory NiTi to provide enhanced flexibility and resistance to cyclic fatigue (24). The V-Taper 2H system includes three primary files that have a 6% taper in the apical 3 mm and then reduce up the shank until MFD is reached at D_{12}. The three files are 20/0.06v, 25/0.06v, and 30/0.06v with MFDs of 0.64, 0.69, and 0.76 mm, respectively. The use of V-Taper 2H has been recommended in the practice of conservative endodontics as its ability to pre-bend facilitates access into contracted access cavities (25).

Minimally Invasive Access and Instrumentation in Endodontics

Minimally invasive endodontic focuses both on the access cavity and instrumentation of the canal system. Minimally invasive dentistry has been defined as the application of “a systematic respect for the original tissue (26).” Key opinion leaders in endodontics have used the terms “minimally invasive” and “conservative” interchangeably to describe the paradigm shift in treatment. The access opening is an essential precursor to chemomechanical debridement of the root canal system, and the steps following the access may be compromised if it is inadequate (27). The objective of a proper endodontic access is to facilitate the complete debridement, irrigation, shaping, cleaning, and filling of the root canal system (28). Modern advancement in instrumentation and equipment provides clinicians with the ability to be more conservative with access openings, thus shifting away from a traditional access opening that prioritizes straight line access and visualization of canals. The endodontic access size as it pertains to remaining tooth structure plays an important role in the restorative prognosis and long-term survival of the tooth (29). A conservative access cavity emphasizes the importance of maintaining as much enamel and dentin as possible. The focus is on the preservation of pericervical dentin which is the dentin 4 mm apical and 4 mm coronal to the crestal bone (5). There is conflicting evidence regarding the effect of a traditional access cavity compared to a conservative access cavity on fracture resistance and stress distribution with regard to the entire tooth (30–33).

Vertical Root Fracture

Vertical root fracture (VRF) is a clinical problem that occurs primarily in endodontically treated teeth (34). It is defined by the American Association of Endodontists as a fracture in the root whereby the fractured segments are incompletely separated; it may occur buccal-lingually or mesial-distally; it may cause an isolated periodontal defect(s) or sinus tract; it may be radiographically evident (35). Canal preparation involves the removal of dentin from canal walls which may compromise the fracture resistance of the roots (36). Lam evaluated NiTi canal preparations compared to hand file preparation and found that NiTi preparations are more likely to be round and smooth thereby reducing the number of canal irregularities that may act as points of stress concentration (37). Rundquist studied the root stress during different phases of root canal treatment (38). It was concluded that during warm vertical obturation, root stress decreases as canal taper increases. After the completion of treatment, stresses are greatest at the cervical portion of the root surface and stresses increase slightly as taper increases. Rundquist suggested that that vertical root fractures initiated at the apex are the result of excessive force during obturation whereas root fractures originating cervically are a product of masticatory forces on the tooth.

Wilcox found that when using cold lateral compaction, there was an increase in spreader induced vertical root fractures with increases in canal enlargement. It has been concluded that the removal of dentin does not always result in increased fracture susceptibility (39). RCT have high success rates at 10 years, but the most common reasons for failure are fracture or restorability (40). With the introduction of supplemental irrigation systems such as the Gentle Wave System (Sonendo, Inc., Laguna

Hills, CA, USA), there will continue to be a discussion among dental professionals as to how endodontic treatment can be carried out with minimal instrumentation of the root canal system (41).

Finite Element Analysis in Dentistry

The finite element method (FEM) is a numerical method of that solves differential equations. A geometric structure is built and divided into small elements that are connected by nodes. There are associated equations that form a finite set of equations that provide information about the stress distributions between the elements and nodes (42). The size, quantity, and arrangement of "finite elements" and nodes impact the accuracy of the results (43). FEM is the mathematical method that provides the foundation for finite element analysis (FEA). The finite element method can be applied in two dimensions (2D) and three dimensions (3D). The finite element method has been used for nearly three decades in studies to perform stress analysis of teeth. Studies have shown that application of a 3D finite element method provides a more accurate analysis than a 2D method in analysis of stresses in teeth (44,45).

FEA is a computer simulation technique that uses the underlying FEM to realistically model stress distribution. Unlike physical methods such as a strain gauge, FEM can quantify stresses and displacement throughout the anatomy of a 3D structure (46). Since the first 3D FEA study in 1983, there have been significant advancements in computer tomography (CT) capabilities and computer-aid-design (CAD) software that have improved the accuracy of FEA in dentistry. In FEA, solid models are created from CT, micro CT, or magnetic resonance image (MRI) datasets. The 2D slices that are obtained from the datasets are segmented using software to develop a 3D rendering of the object being analyzed. In many cases, small irregularities may occur during segmentation and their accuracy must be verified prior to completing analysis. After segmentation, a mesh is created from the solid model. The mesh is based off discretization which is the mathematical process that allows for numerical evaluation of the model. All steps including segmentation, processing, and meshing are carried out using sophisticated software that is developed for engineering applications. The resulting mesh is then loaded into a FEA software. Load, boundary conditions, and material properties are applied to the model. Stress distribution can then be analyzed both qualitatively and quantitatively (46).

It's important to note that FEA has limitations. The accuracy of FEA modeling depends on the accuracy in simulating the geometry and surface structure of the sample. FEA in dentistry and teeth is limited to the confines of the model and extent of the information included. Chewing functions and movements can only be simulated under static loading where properties are set as isotropic and linearly elastic. The assumptions made during the modeling and the limitations of the software used limit the extent that FEA can mimic a clinical situation (47).

While keeping in mind its limitations, there are numerous benefits to using FEA, as it allows for the location, magnitude, and direction of applied forces to be analyzed and adjusted to locate stress points that can be theoretically measured (48). Additionally, the physical properties of the materials can be reassigned or modified, and there is no physical destruction of the sample, making simulations easily repeatable (49). With adequate understanding of the limitations of FEA, advancements in technology have made it a reliable method for primary testing and would be most beneficial when supplemented with a clinical experiment.

Materials and Methods

Two identical three dimensionally (3-D) printed mandibular plastic molars (Tooth #19) were used in this study (Acadental Endo 3DP). Both teeth were 3-D printed with a standardized conventional access opening allowing for straight line access to the mesial and distal canals. Both teeth were mounted in ModuPRO carriers and inserted into the ModuPRO manikin (Acadental). Working length was measured in each tooth with a size 15-k file (Roydent, Johnson City, TN) and confirmed with a radiograph 0.5 mm short of the radiographic apex. One tooth was instrumented with ProTaper Gold (Dentsply Sirona) to F2 (25/0.08v progressive taper) in the mesial canals and F3 (30/0.09v progressive taper), in distal canals using manufacturer protocol. The other instrumented tooth was instrumented with V-Taper 2H System (SS White) to 25/0.06v (minimal taper) in mesial canals and 30/0.06v (minimal taper) in the distal canals by manufacturer protocol.

The canals were obturated with sealer and gutta percha to provide contrast for scanning. All procedures were completed in a manikin using a microscope to simulate clinical treatment. After the preparation procedures were finished, each model was digitized separately using a high-resolution micro CT-Scan. The micro CT-Scan and STL reconstruction were completed by Exact Metrology (Brookfield, WI) using a GOM CT scanner at 25-µM voxel size, 150 kV Target X-Ray Voltage, 40 W X-Ray Target Power, Exposure Time: 1500 milliseconds, 750 exposure and GOM Inspect software (Braunschweig, Germany).

The high-resolution STL files, created by micro-CT scanning machine, were imported to the 3-matic software (3-matic Medical v 13, Materialise N. V., Belgium) to be prepared for the finite element analysis, (figure 1, a). The three-dimensional models of the tooth and the filling were intensively treated through several tools in order to selectively reduce mesh density, smoothen, and improve polygonal mesh quality for finite element analysis (figure 2, a). Afterward, the periodontal ligament (PDL) was designed as an offset shell surrounding the root surface from the estimated cemento-enamel junction (CEJ) to the root apex (figure 1, b). In addition, the bone was modeled by creating a cross-section outline on a 2-D sketch then extracting to form the desired volume using sketch and design modules of the software (figure 2, b). In order to have two models representing the composite filling and gutta percha, the filling 3D model was separated at the floor of the pulp chamber with a single body for composite filling bodies for gutta percha. Afterwards, a non-manifold assembly was created from the 3D models of the previous components.

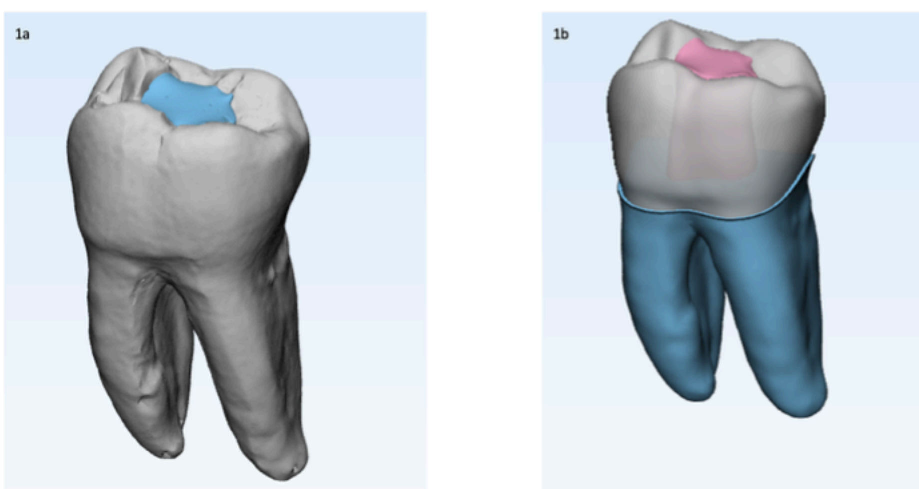

Figure 1:

a. *3D model of the 3D-printed tooth with raw high-resolution mesh polygons including its filling materials*
b. *3D model of the tooth and filling materials after modification in 3-matic software and creation of the PDL model.*

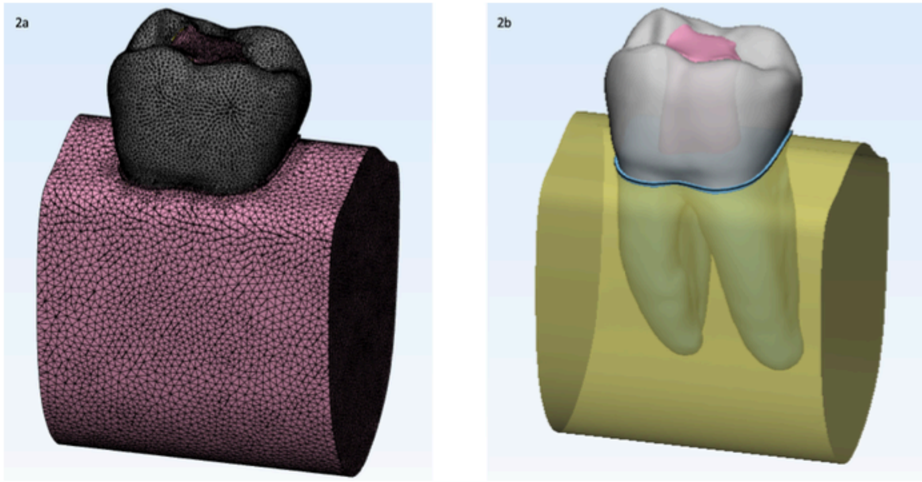

Figure 2:

a. *Surface details of the polygon 3D model after treatment and refinement at the fine and contact areas between objects.*
b. *3D model after modeling the bone to be added to the assembly as created by*

To enhance the accuracy of the analysis, the model of the Pro-Taper tooth and filling was duplicated, and a registration process was performed between the duplicate and the V-taper tooth model followed by replacing the gutta percha part of the duplicate model with that of the V-taper model. Accordingly, only the root canal filling part became the difference between the Pro-taper and the V-taper models (figure 3, 4). Finally, the non-manifold assembly files of the two groups were converted to a volume mesh with a suitable element growth rate to keep element size within acceptable range (figure 5). The volume mesh quality was analyzed to check if the quality meets the finite element software and resolve any errors generated during conversion. The volume mesh was then exported as a finite element mesh file.

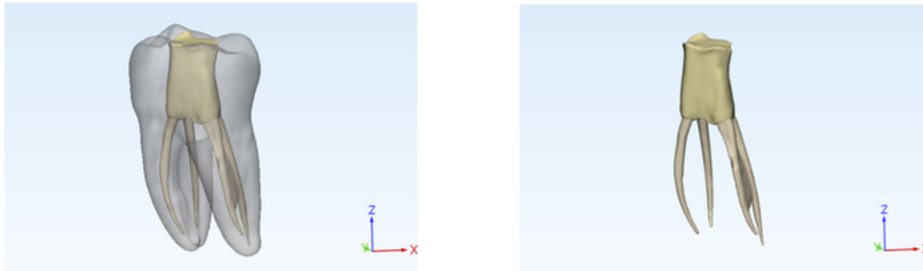

***Figure 3**: 3D models of the Pro-Taper tooth and their corresponding fillings (composite & gutta percha)*

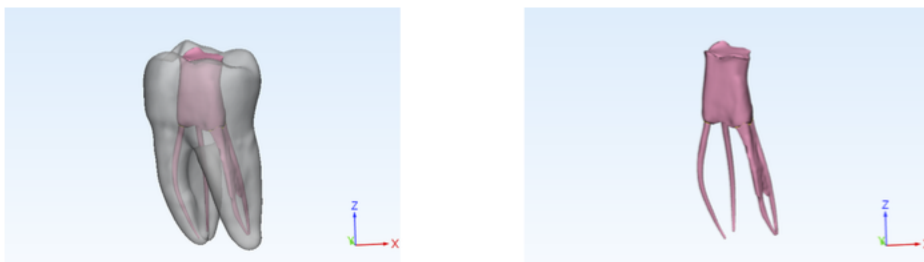

***Figure 4**: 3D models of the V-taper tooth and filling after registration and fitting to duplicate composite filling added.*

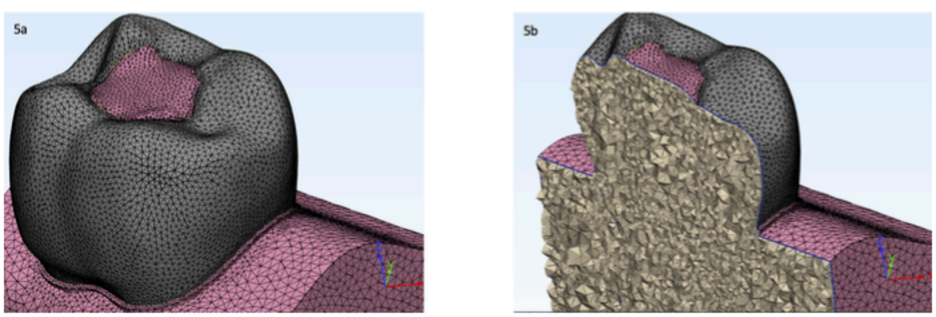

***Figure 5**:*

a. *Closer view of the surface details and refinement before creation of the volume mesh.*
b. *Volume mesh created with suitable growth rate as shown in the cross-cut image with smaller elements at the object's surfaces and contact areas.*

The exported files were imported to the finite element software (ANSYS Workbench *v* 14, Canonsburg, PA, USA) as finite element modeler files. As the study was considered a linear problem and all bodies were considered isotropic, each body has one value for the elastic modulus and Poisson's ratio. The material properties of each body were assigned from the pre-customized engineering library using data from literatures (Table 1,) (50–57).

	Elastic modulus-E (MPa)	Poisson's ratio (υ)
Dentin	18000	0.31
Bone	1370	0.3
PDL	50	0.45
Composite	15800	0.24
Gutta percha	0.14	0.32

Table 1: *Material properties assigned for different bodies of the bar systems.*

The mesh of the imported parts showed total element number (1624508) and nodes (292326) using tetrahedron element (solid185) which is suitable for linear materials and studies (figure 6). The contact type between all parts was bonded contact as no sliding is allowed at the interface to show bonding between contact parts and to enhance calculations.

A two hundred Newton (200 N) force was applied as a nodal force directed perpendicularly (in -Z direction) on the buccal cusps and central fossa while the constraints were applied to permit zero degree of freedom from both mesial and distal sides of the bone object, as a boundary condition. The stress load of 200 N is unlikely to cause fracture in all models, but provides a simulation of normal chewing function.

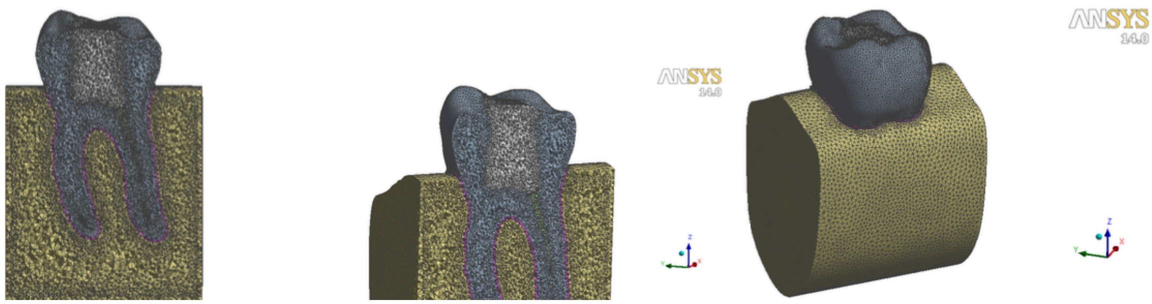

Figure 6*: 3D volume mesh created by tetrahedron elements imported to the finite element module of the finite element software (ANSYS v 14)*

The finite element solution planned to include the equivalent (Von Mises) stress (σ) and total deformation of the tooth structure with and without composite filling to simulate a period of temporization. Von Mises stress criteria is used to estimate the yield of ductile materials and has been used to evaluate failure in human teeth (58). Von Mises equivalent stress was calculated in each simulation. Total deformation is the change in shape of the object as a result of the stress in each area. Both outcome measures were checked at the estimated cemento-enamel junction (CEJ) and at (1,2,3,4,5 mm) from the CEJ by creating six construction geometry surfaces. All the data was collected and tabulated, and figures with color-scale bar legends were developed for analysis and comparison. An isometric view was used to visualize the four canals and the stress distribution throughout the tooth for qualitative analysis.

RESULTS

In simulations with and without a resin access restoration, the Pro-Taper Gold models had higher maximum stress values than that of the V-Taper 2H groups (Table 2, 3, 4, and 5). The Pro-Taper tooth that was not filled with composite resin had a higher maximum stress value (19.86 MPa) than did the model with the access filled with resin (16.87 MPa). Between the V-Taper 2H models, the model in which the access was not filled with composite resin (12.73 MPa) had a lower maximum stress value than did the model filled with resin (14.19 MPa). Between the two simulation groups, the models where the accesses were left empty had higher total deformation values than did the models with a filled access. Under a 200-N multipoint load, the Von Mises stress was higher in the Pro-Taper Gold prepared models than in the V-Taper 2H prepared models. The greatest stress values were found in the pericervical dentin, and stresses decreased apically through the root. In all models, total deformation values were highest in the clinical crown on the buccal aspect of the tooth.

Table 2: *Von Mises stress with composite filling in place in (MPa)*

		Full tooth	**0 mm**	**1 mm**	**2 mm**	**3 mm**	**4 mm**	**5 mm**
Pro-taper	Maximum Ō	16.868	9.0089	9.3787	8.1795	7.5786	7.4644	7.4646
	Minimum Ō	0.15174	0.19631	0.27999	0.27943	0.2148	0.20279	0.37367
V-taper	Maximum Ō	14.185	5.0602	5.2507	4.6141	4.4592	4.2914	4.3267
	Minimum Ō	8.5654e-002	0.175	0.14715	0.18342	0.11577	0.10935	0.18011

* 0,1,2.....5 mm : is distance from CEJ

Table 3: *Total Deformation with composite filling in place in (mm)*

		Full tooth	**0 mm**	**1 mm**	**2 mm**	**3 mm**	**4 mm**	**5 mm**
Pro-taper	Maximum	2.4347e-002	1.912e-002	1.827e-002	1.733e-002	1.661e-002	1.598e-002	1.536e-002
	Minimum	6.757e-003	8.793e-003	8.127e-003	7.578e-003	7.194e-003	6.938e-003	6.804e-003
V-taper	Maximum	1.5175e-002	1.1514e-002	1.0862e-002	1.0317e-002	9.8446e-003	9.4292e-003	9.0892e-003
	Minimum	4.0298e-003	5.3017e-003	4.8875e-003	4.5464e-003	4.3018e-003	4.1422e-003	4.0584e-003

Table 4: *Von Mises stress without composite filling in place in (MPa)*

		Full tooth	**0 mm**	**1 mm**	**2 mm**	**3 mm**	**4 mm**	**5 mm**
Pro-taper	Maximum Ō	19.855	13.176	12.973	11.379	10.673	10.099	9.713
	Minimum Ō	0.10217	0.29892	0.44006	0.35949	0.52194	0.82012	0.95936
V-taper	Maximum Ō	12.732	7.9251	7.8086	7.1519	6.7759	6.3073	5.9445
	Minimum Ō	7.252e-002	0.12335	0.24549	0.2755	0.35256	0.5126	0.69747

Table 5: *Total Deformation without composite filling in place in (mm)*

		Full tooth	**0 mm**	**1 mm**	**2 mm**	**3 mm**	**4 mm**	**5 mm**
Pro-taper	Maximum	3.5088e-002	2.4127e-002	2.2686e-002	2.1153e-002	1.9989e-002	1.898e-002	1.8014e-002
	Minimum	4.1872e-003	9.5484e-003	8.0512e-003	6.7275e-003	5.6515e-003	4.8428e-003	4.3493e-003
V-taper	Maximum	2.3435e-002	1.5185e-002	1.4059e-002	1.303e-002	1.2231e-002	1.1554e-002	1.0912e-002
	Minimum	2.1564e-003	6.1145e-003	5.0702e-003	4.1325e-003	3.3383e-003	2.711e-003	2.301e-003

***Figure 7**: Von Mises Stress with composite filling in place in (MPa), Pro-Taper (left) and V-Taper (right)*

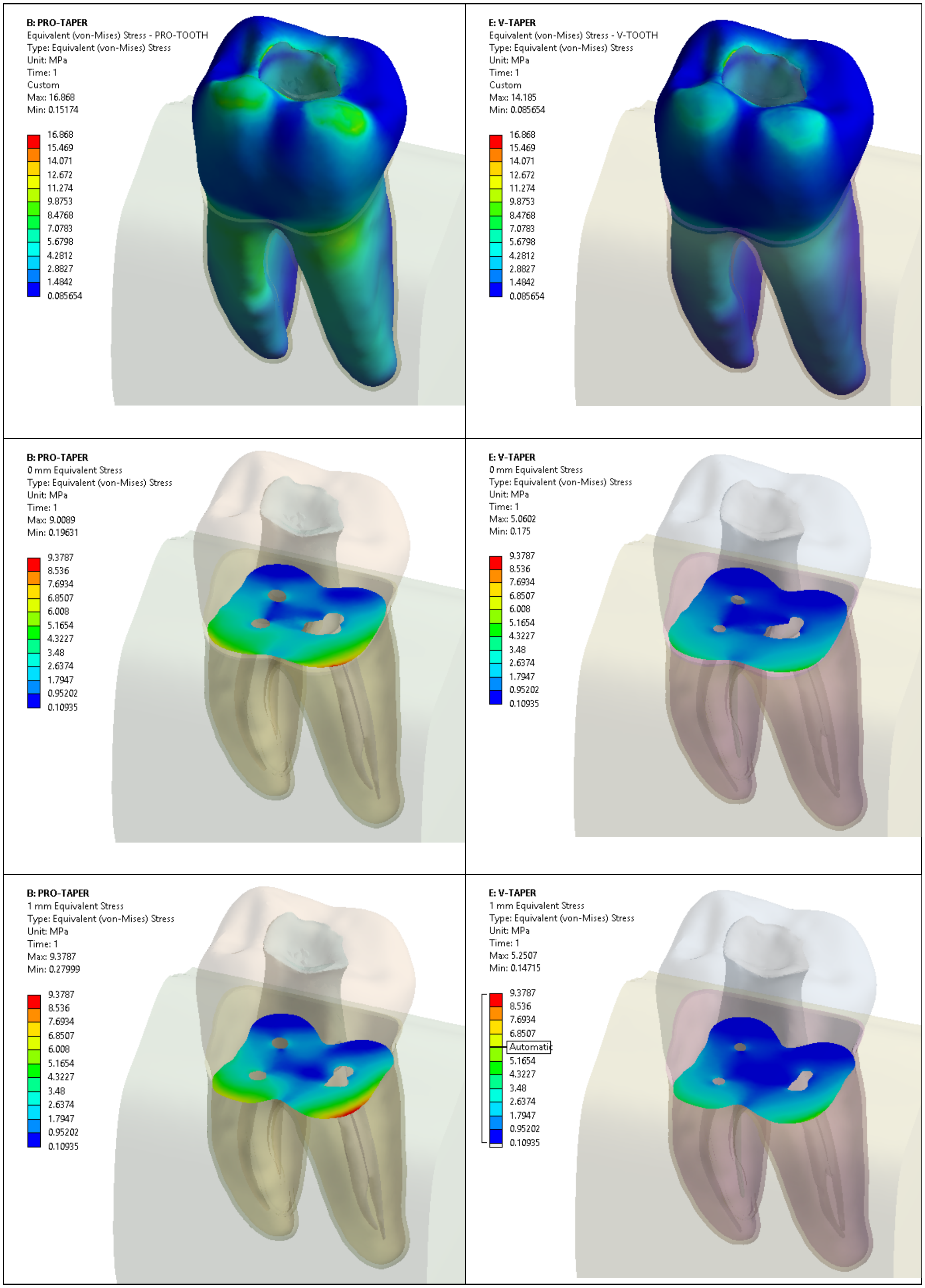

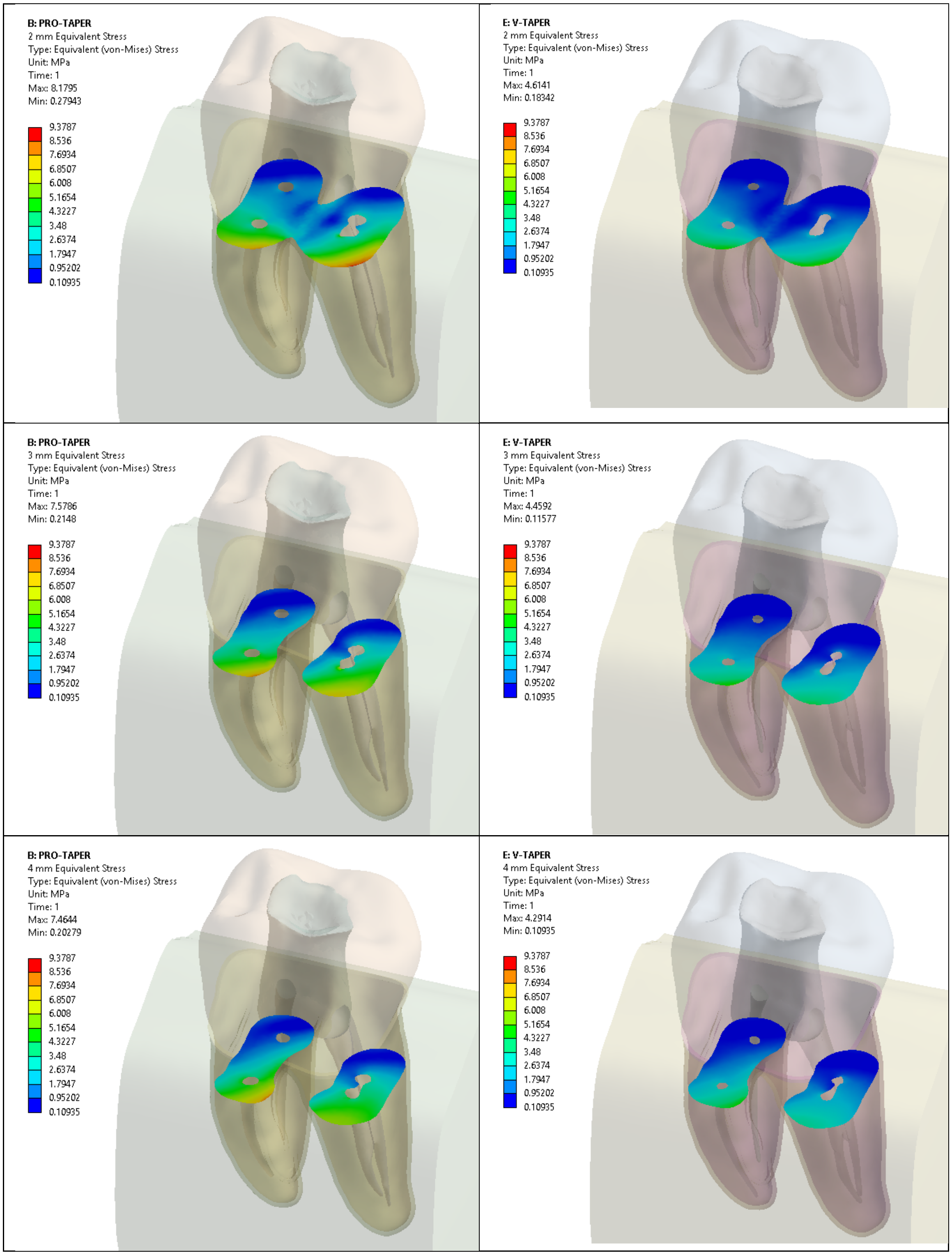
B: PRO-TAPER
2 mm Equivalent Stress
Type: Equivalent (von-Mises) Stress
Unit: MPa
Time: 1
Max: 8.1795
Min: 0.27943
9.3787
8.536
7.6934
6.8507
6.008
5.1654
4.3227
3.48
2.6374
1.7947
0.95202
0.10935
E: V-TAPER
2 mm Equivalent Stress
Type: Equivalent (von-Mises) Stress
Unit: MPa
Time: 1
Max: 4.6141
Min: 0.18342
9.3787
8.536
7.6934
6.8507
6.008
5.1654
4.3227
3.48
2.6374
1.7947
0.95202
0.10935
B: PRO-TAPER
3 mm Equivalent Stress
Type: Equivalent (von-Mises) Stress
Unit: MPa
Time: 1
Max: 7.5786
Min: 0.2148
9.3787
8.536
7.6934
6.8507
6.008
5.1654
4.3227
3.48
2.6374
1.7947
0.95202
0.10935
E: V-TAPER
3 mm Equivalent Stress
Type: Equivalent (von-Mises) Stress
Unit: MPa
Time: 1
Max: 4.4592
Min: 0.11577
9.3787
8.536
7.6934
6.8507
6.008
5.1654
4.3227
3.48
2.6374
1.7947
0.95202
0.10935
B: PRO-TAPER
4 mm Equivalent Stress
Type: Equivalent (von-Mises) Stress
Unit: MPa
Time: 1
Max: 7.4644
Min: 0.20279
9.3787
8.536
7.6934
6.8507
6.008
5.1654
4.3227
3.48
2.6374
1.7947
0.95202
0.10935
E: V-TAPER
4 mm Equivalent Stress
Type: Equivalent (von-Mises) Stress
Unit: MPa
Time: 1
Max: 4.2914
Min: 0.10935
9.3787
8.536
7.6934
6.8507
6.008
5.1654
4.3227
3.48
2.6374
1.7947
0.95202
0.10935

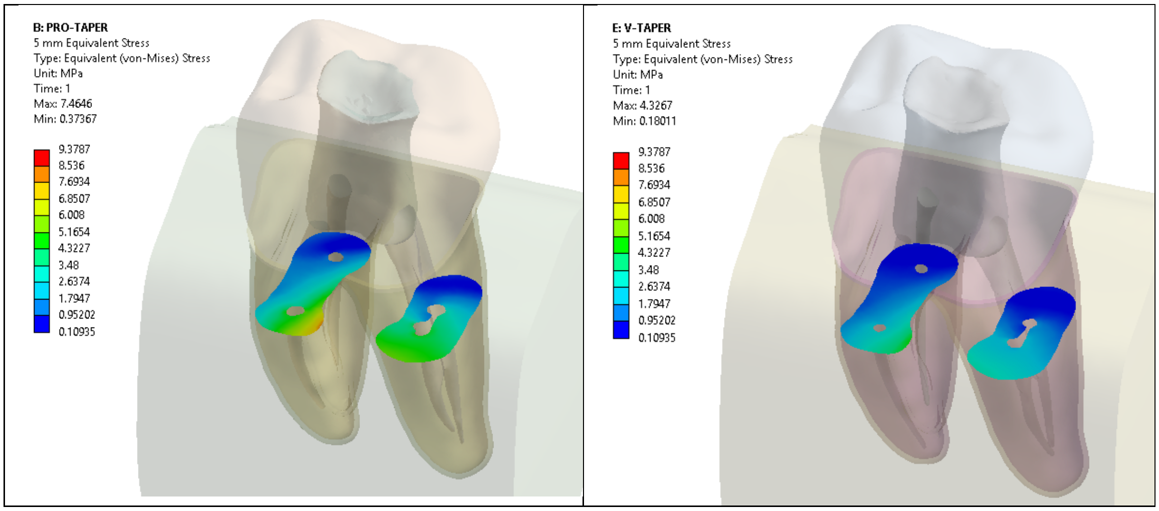

Figure 8*: Total Deformation with composite filling in place in (MPa), Pro-Taper (left) and V-Taper (right)*

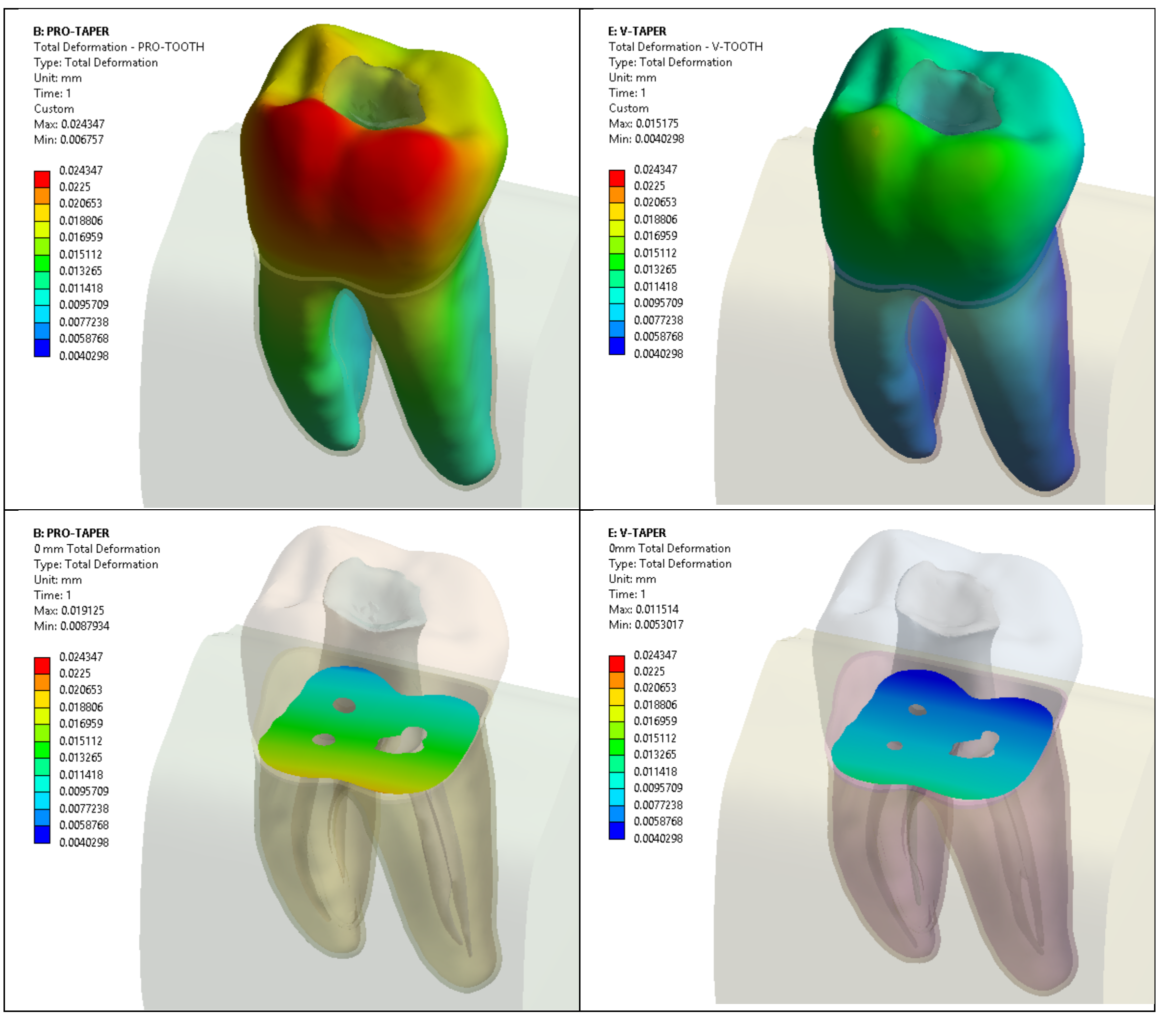

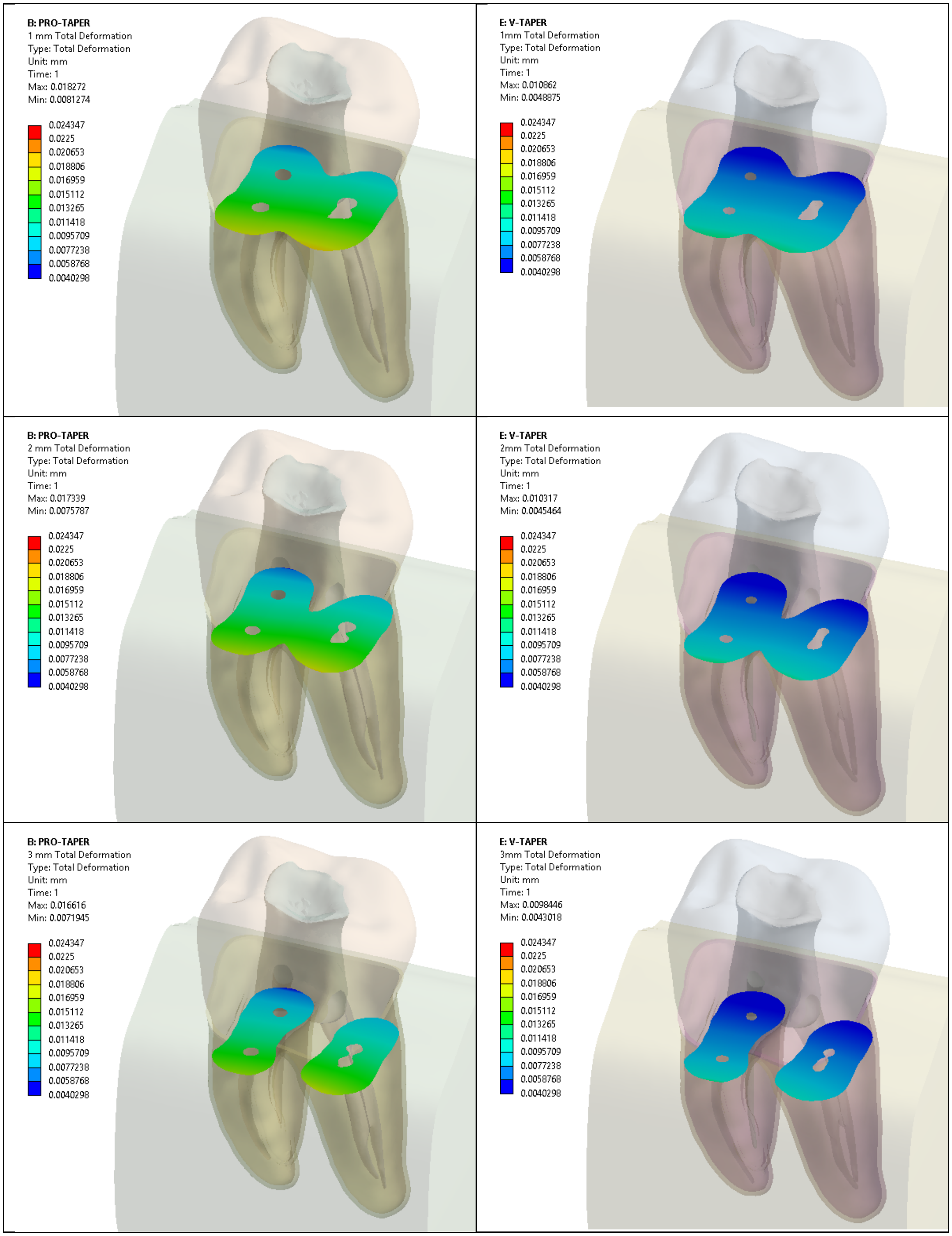
B: PRO-TAPER
1 mm Total Deformation
Type: Total Deformation
Unit: mm
Time: 1
Max: 0.018272
Min: 0.0081274
0.024347
0.0225
0.020653
0.018806
0.016959
0.015112
0.013265
0.011418
0.0095709
0.0077238
0.0058768
0.0040298
E: V-TAPER
1mm Total Deformation
Type: Total Deformation
Unit: mm
Time: 1
Max: 0.010862
Min: 0.0048875
0.024347
0.0225
0.020653
0.018806
0.016959
0.015112
0.013265
0.011418
0.0095709
0.0077238
0.0058768
0.0040298
B: PRO-TAPER
2 mm Total Deformation
Type: Total Deformation
Unit: mm
Time: 1
Max: 0.017339
Min: 0.0075787
0.024347
0.0225
0.020653
0.018806
0.016959
0.015112
0.013265
0.011418
0.0095709
0.0077238
0.0058768
0.0040298
E: V-TAPER
2mm Total Deformation
Type: Total Deformation
Unit: mm
Time: 1
Max: 0.010317
Min: 0.0045464
0.024347
0.0225
0.020653
0.018806
0.016959
0.015112
0.013265
0.011418
0.0095709
0.0077238
0.0058768
0.0040298
B: PRO-TAPER
3 mm Total Deformation
Type: Total Deformation
Unit: mm
Time: 1
Max: 0.016616
Min: 0.0071945
0.024347
0.0225
0.020653
0.018806
0.016959
0.015112
0.013265
0.011418
0.0095709
0.0077238
0.0058768
0.0040298
E: V-TAPER
3mm Total Deformation
Type: Total Deformation
Unit: mm
Time: 1
Max: 0.0098446
Min: 0.0043018
0.024347
0.0225
0.020653
0.018806
0.016959
0.015112
0.013265
0.011418
0.0095709
0.0077238
0.0058768
0.0040298

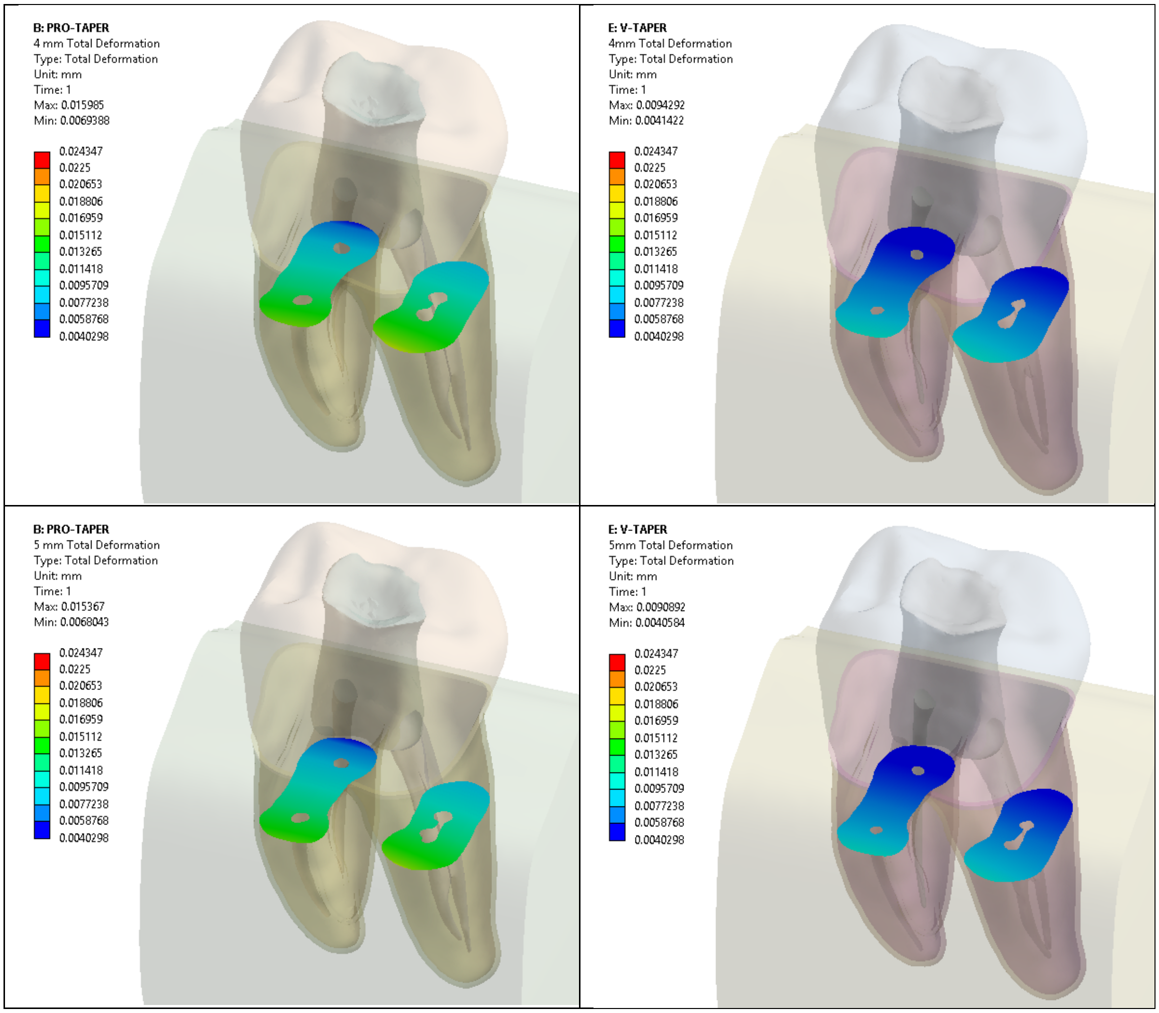

Figure 9*: Von Mises Stress without composite filling in place in (MPa), Pro-Taper (left) and V-Taper (right)*

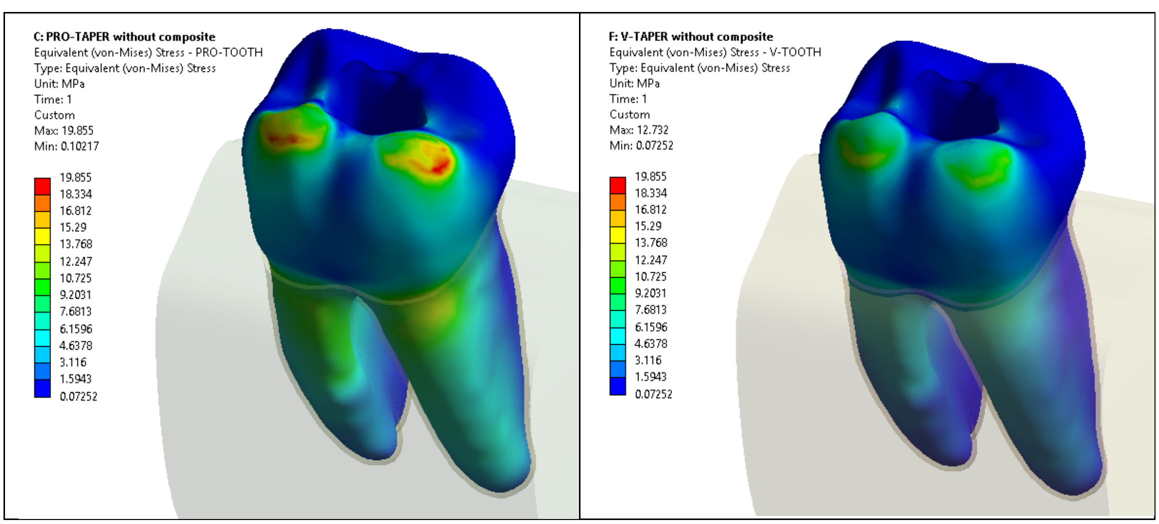

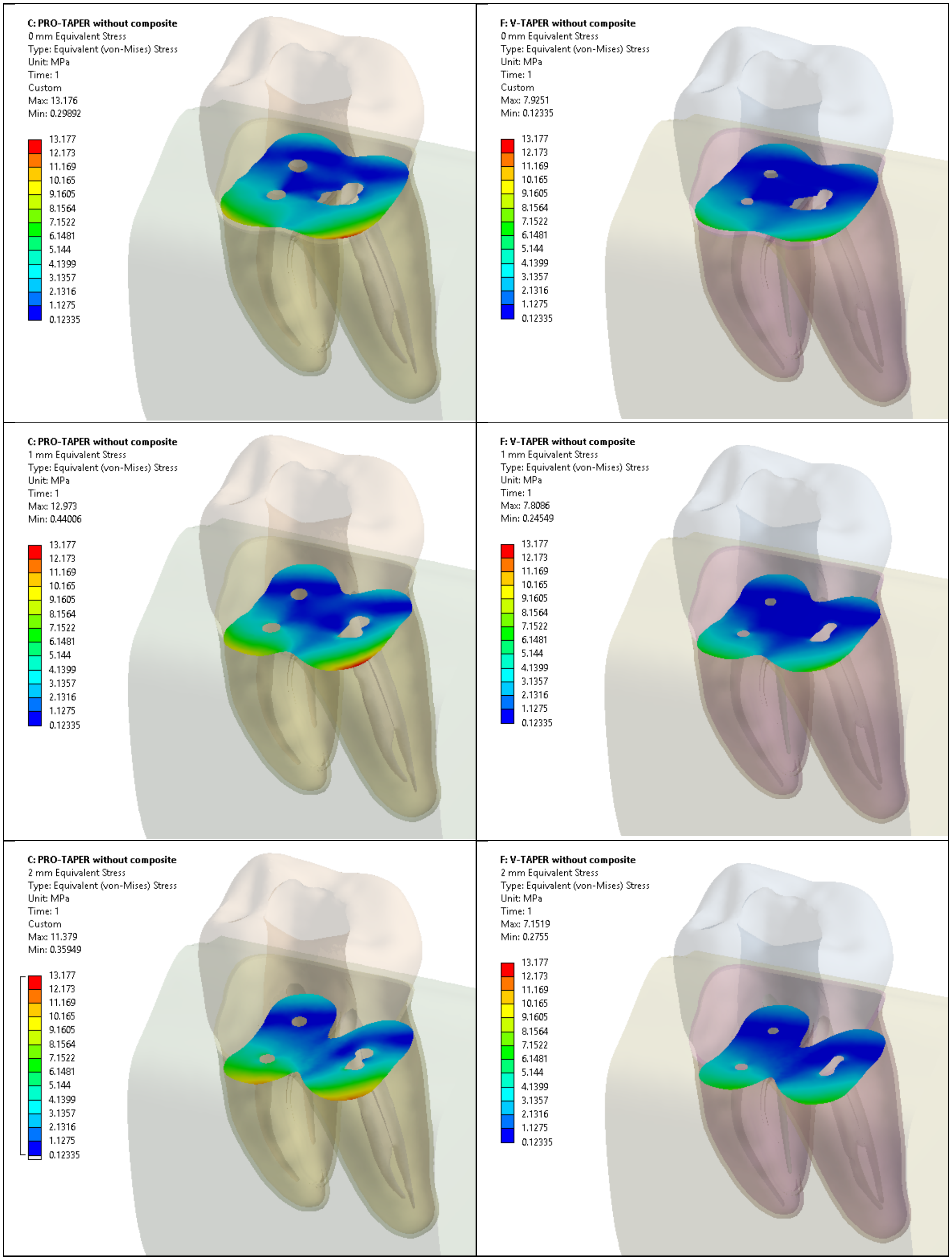
C: PRO-TAPER without composite
0 mm Equivalent Stress
Type: Equivalent (von-Mises) Stress
Unit: MPa
Time: 1
Custom
Max: 13.176
Min: 0.29892
13.177
12.173
11.169
10.165
9.1605
8.1564
7.1522
6.1481
5.144
4.1399
3.1357
2.1316
1.1275
0.12335
F: V-TAPER without composite
0 mm Equivalent Stress
Type: Equivalent (von-Mises) Stress
Unit: MPa
Time: 1
Custom
Max: 7.9251
Min: 0.12335
13.177
12.173
11.169
10.165
9.1605
8.1564
7.1522
6.1481
5.144
4.1399
3.1357
2.1316
1.1275
0.12335
C: PRO-TAPER without composite
1 mm Equivalent Stress
Type: Equivalent (von-Mises) Stress
Unit: MPa
Time: 1
Max: 12.973
Min: 0.44006
13.177
12.173
11.169
10.165
9.1605
8.1564
7.1522
6.1481
5.144
4.1399
3.1357
2.1316
1.1275
0.12335
F: V-TAPER without composite
1 mm Equivalent Stress
Type: Equivalent (von-Mises) Stress
Unit: MPa
Time: 1
Max: 7.8086
Min: 0.24549
13.177
12.173
11.169
10.165
9.1605
8.1564
7.1522
6.1481
5.144
4.1399
3.1357
2.1316
1.1275
0.12335
C: PRO-TAPER without composite
2 mm Equivalent Stress
Type: Equivalent (von-Mises) Stress
Unit: MPa
Time: 1
Custom
Max: 11.379
Min: 0.35949
13.177
12.173
11.169
10.165
9.1605
8.1564
7.1522
6.1481
5.144
4.1399
3.1357
2.1316
1.1275
0.12335
F: V-TAPER without composite
2 mm Equivalent Stress
Type: Equivalent (von-Mises) Stress
Unit: MPa
Time: 1
Max: 7.1519
Min: 0.2755
13.177
12.173
11.169
10.165
9.1605
8.1564
7.1522
6.1481
5.144
4.1399
3.1357
2.1316
1.1275
0.12335

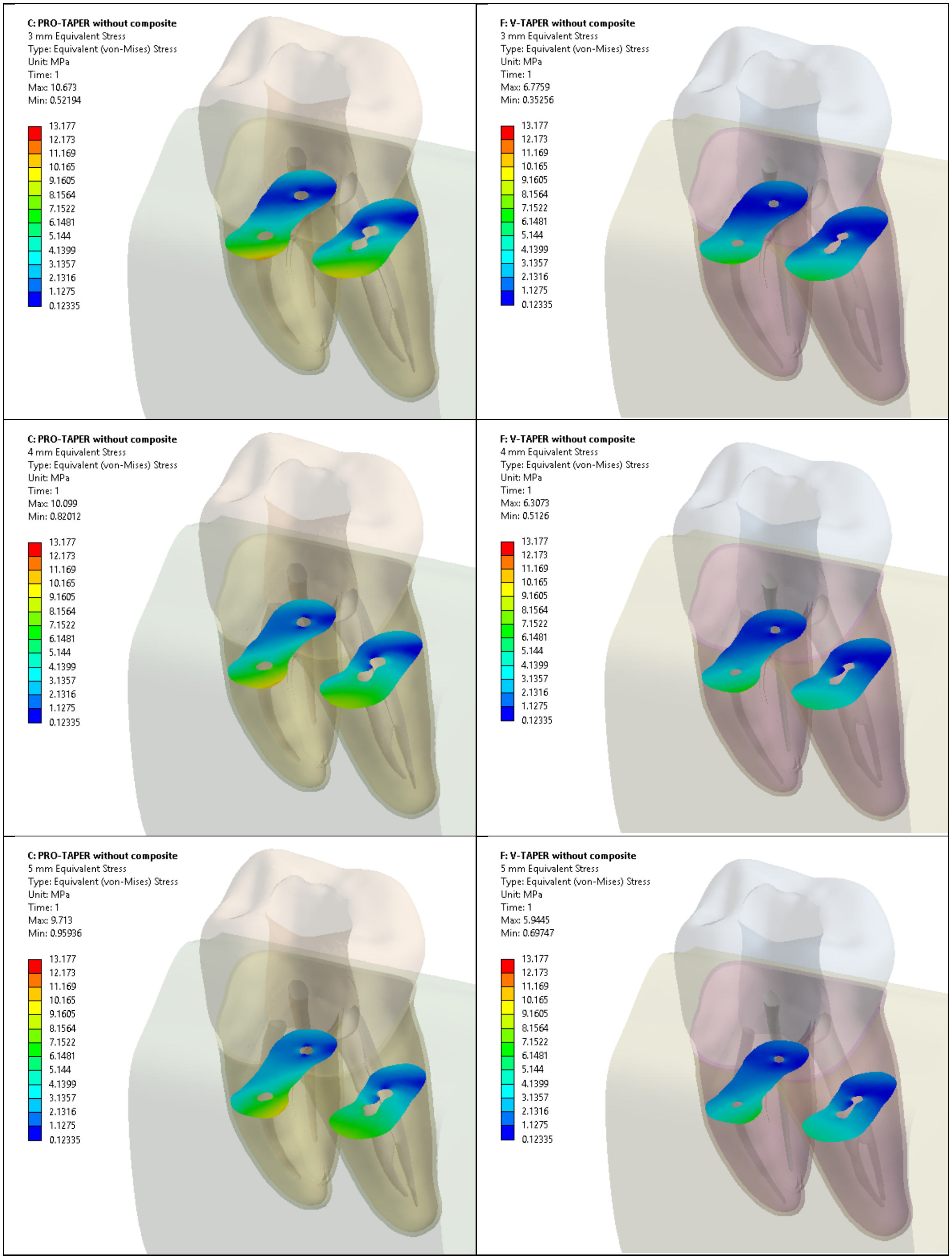
C: PRO-TAPER without composite
3 mm Equivalent Stress
Type: Equivalent (von-Mises) Stress
Unit: MPa
Time: 1
Max: 10.673
Min: 0.52194
13.177
12.173
11.169
10.165
9.1605
8.1564
7.1522
6.1481
5.144
4.1399
3.1357
2.1316
1.1275
0.12335
F: V-TAPER without composite
3 mm Equivalent Stress
Type: Equivalent (von-Mises) Stress
Unit: MPa
Time: 1
Max: 6.7759
Min: 0.35256
13.177
12.173
11.169
10.165
9.1605
8.1564
7.1522
6.1481
5.144
4.1399
3.1357
2.1316
1.1275
0.12335
C: PRO-TAPER without composite
4 mm Equivalent Stress
Type: Equivalent (von-Mises) Stress
Unit: MPa
Time: 1
Max: 10.099
Min: 0.82012
13.177
12.173
11.169
10.165
9.1605
8.1564
7.1522
6.1481
5.144
4.1399
3.1357
2.1316
1.1275
0.12335
F: V-TAPER without composite
4 mm Equivalent Stress
Type: Equivalent (von-Mises) Stress
Unit: MPa
Time: 1
Max: 6.3073
Min: 0.5126
13.177
12.173
11.169
10.165
9.1605
8.1564
7.1522
6.1481
5.144
4.1399
3.1357
2.1316
1.1275
0.12335
C: PRO-TAPER without composite
5 mm Equivalent Stress
Type: Equivalent (von-Mises) Stress
Unit: MPa
Time: 1
Max: 9.713
Min: 0.95936
13.177
12.173
11.169
10.165
9.1605
8.1564
7.1522
6.1481
5.144
4.1399
3.1357
2.1316
1.1275
0.12335
F: V-TAPER without composite
5 mm Equivalent Stress
Type: Equivalent (von-Mises) Stress
Unit: MPa
Time: 1
Max: 5.9445
Min: 0.69747
13.177
12.173
11.169
10.165
9.1605
8.1564
7.1522
6.1481
5.144
4.1399
3.1357
2.1316
1.1275
0.12335

Figure 10: *Total Deformation without composite filling in place in (MPa), Pro Taper (left) and V-Taper (right)*

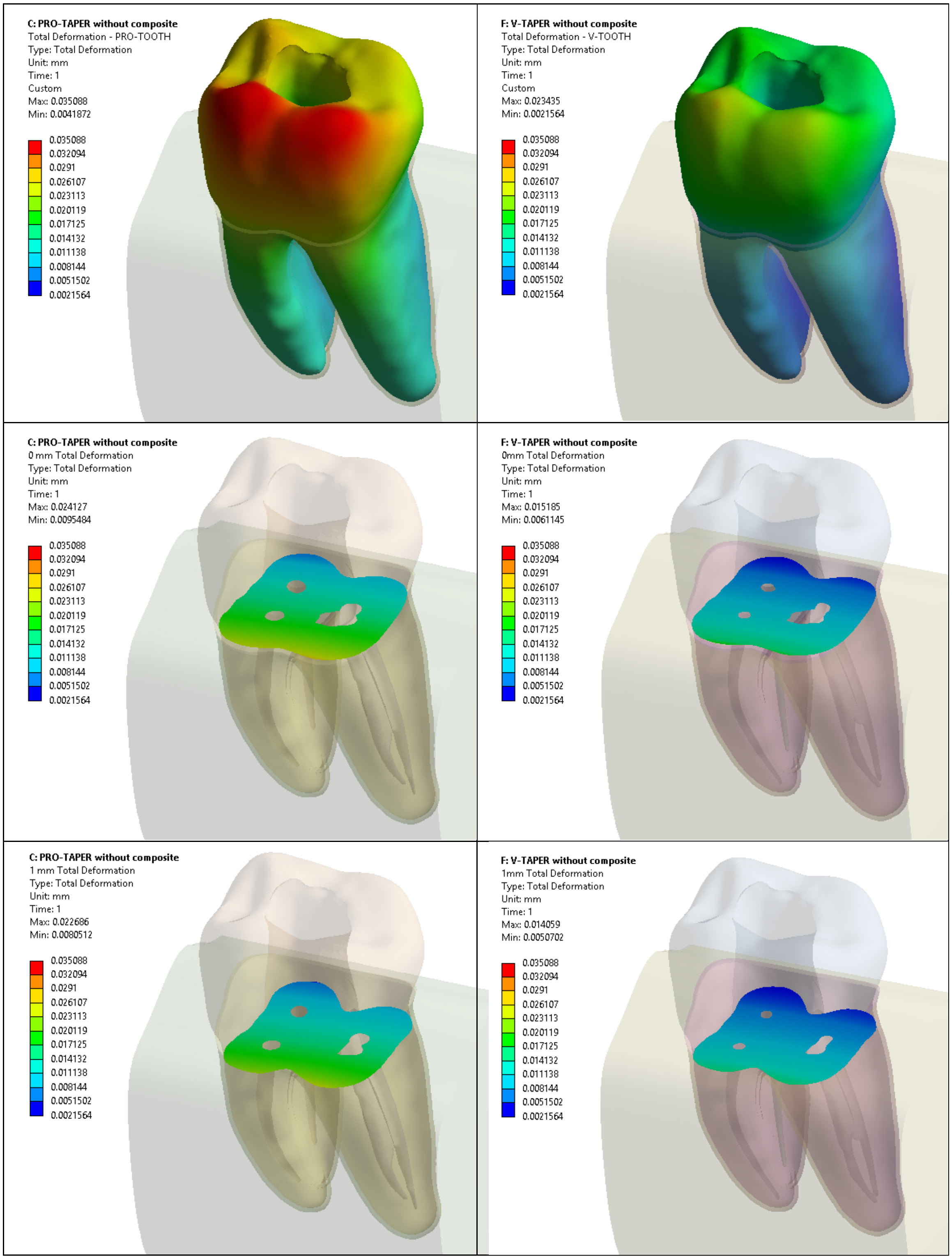

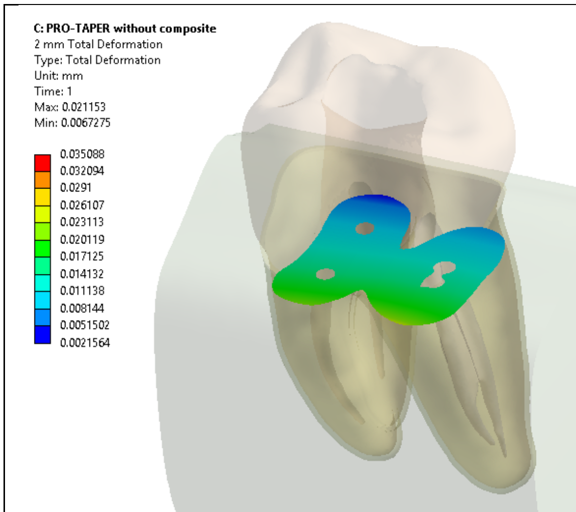
C: PRO-TAPER without composite
2 mm Total Deformation
Type: Total Deformation
Unit: mm
Time: 1
Max: 0.021153
Min: 0.0067275
0.035088
0.032094
0.0291
0.026107
0.023113
0.020119
0.017125
0.014132
0.011138
0.008144
0.0051502
0.0021564

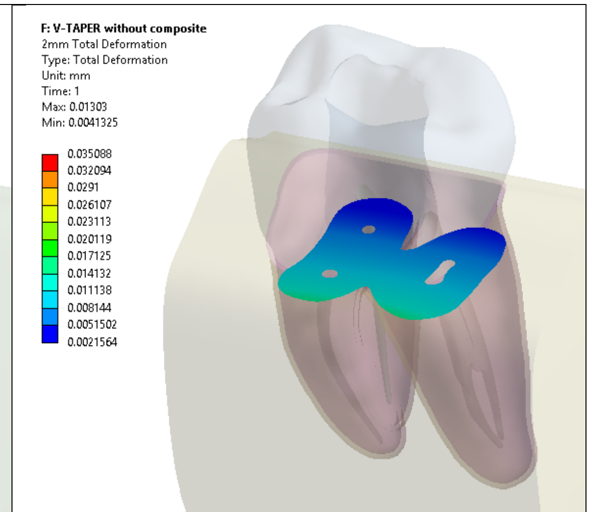
F: V-TAPER without composite
2mm Total Deformation
Type: Total Deformation
Unit: mm
Time: 1
Max: 0.01303
Min: 0.0041325
0.035088
0.032094
0.0291
0.026107
0.023113
0.020119
0.017125
0.014132
0.011138
0.008144
0.0051502
0.0021564

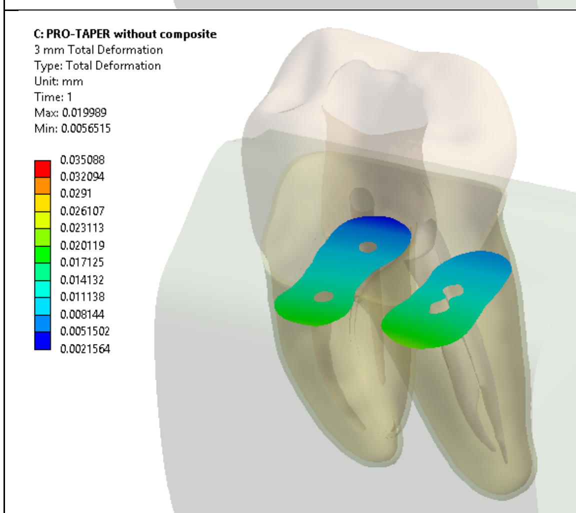
C: PRO-TAPER without composite
3 mm Total Deformation
Type: Total Deformation
Unit: mm
Time: 1
Max: 0.019989
Min: 0.0056515
0.035088
0.032094
0.0291
0.026107
0.023113
0.020119
0.017125
0.014132
0.011138
0.008144
0.0051502
0.0021564

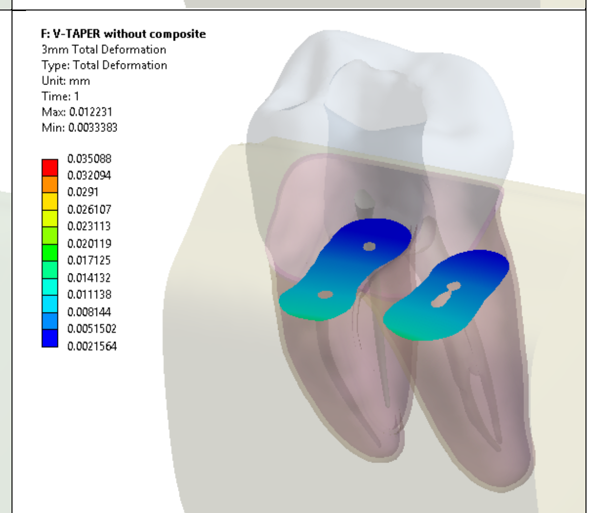
F: V-TAPER without composite
3mm Total Deformation
Type: Total Deformation
Unit: mm
Time: 1
Max: 0.012231
Min: 0.0033383
0.035088
0.032094
0.0291
0.026107
0.023113
0.020119
0.017125
0.014132
0.011138
0.008144
0.0051502
0.0021564

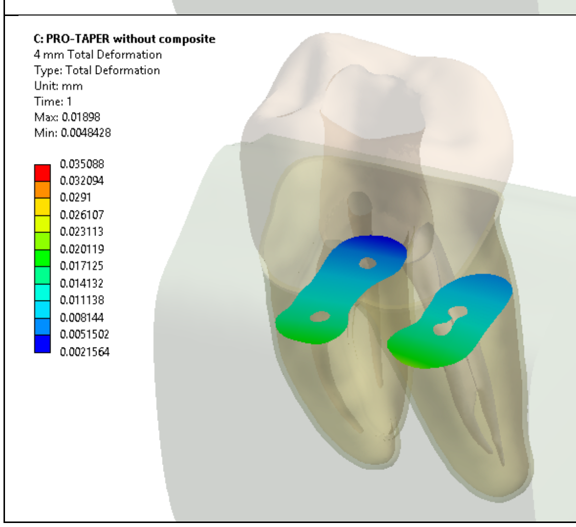
C: PRO-TAPER without composite
4 mm Total Deformation
Type: Total Deformation
Unit: mm
Time: 1
Max: 0.01898
Min: 0.0048428
0.035088
0.032094
0.0291
0.026107
0.023113
0.020119
0.017125
0.014132
0.011138
0.008144
0.0051502
0.0021564

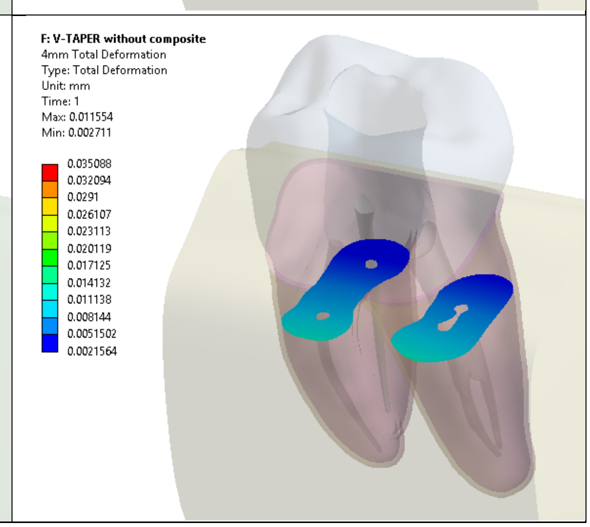
F: V-TAPER without composite
4mm Total Deformation
Type: Total Deformation
Unit: mm
Time: 1
Max: 0.011554
Min: 0.002711
0.035088
0.032094
0.0291
0.026107
0.023113
0.020119
0.017125
0.014132
0.011138
0.008144
0.0051502
0.0021564

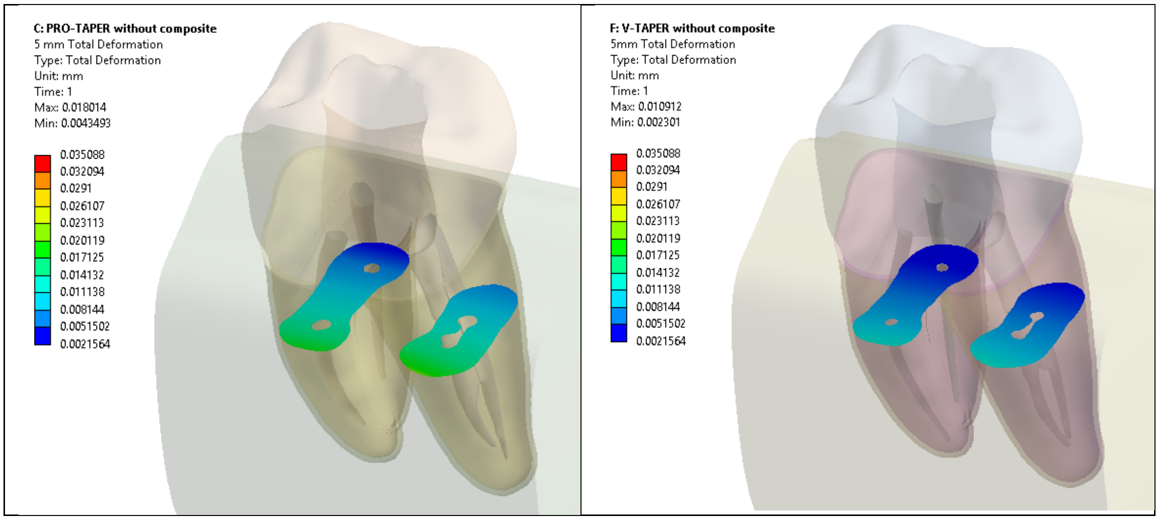
C: PRO-TAPER without composite
5 mm Total Deformation
Type: Total Deformation
Unit: mm
Time: 1
Max: 0.018014
Min: 0.0043493
0.035088
0.032094
0.0291
0.026107
0.023113
0.020119
0.017125
0.014132
0.011138
0.008144
0.0051502
0.0021564
F: V-TAPER without composite
5mm Total Deformation
Type: Total Deformation
Unit: mm
Time: 1
Max: 0.010912
Min: 0.002301
0.035088
0.032094
0.0291
0.026107
0.023113
0.020119
0.017125
0.014132
0.011138
0.008144
0.0051502
0.0021564

DISCUSSION

The primary objective of this study was to determine if the preparation of the root canal system using a minimally tapered file compared to a progressively tapered file affects the stress distribution in a mandibular molar. A mandibular molar was chosen for assessment due to its common indication for endodontic treatment and high incidence of fracture among all teeth (59,60). Additionally, the risk of strip perforation in the mesial canals is an important consideration when treating mandibular molars (61). Two identical teeth were used for independent preparations, and software allowed for the use of one standard external mesh to provide two samples for comparison using FEA.

There are several *in vitro* studies investigating the influence of access design and size on fracture resistance. There are contradicting beliefs regarding the effect of access size on fracture resistance. Ozyurek found that a traditional access does not improve fracture resistance compared to a contracted access in a tooth with a class II restoration (32). Multiple studies comparing a conservative access to a traditional access have found that traditional access cavities may render a tooth more susceptible to fracture than those with a conservative access (62–65). The only systematic review discussing the role of access designs determined that there is no evidence to support a contracted access over a traditional access (66).

In order to only assess the variable of canal taper, a conventional access was used in this study and the teeth were printed with the access made. One of the benefits of FEA is the ability to change material properties within a given model. In order to assess the influence of the resin restoration that was placed in the access cavity, each model was also assessed without a restoration to simulate an open access or if a cotton pellet and temporary restoration were placed at the conclusion of treatment. The results of this analysis suggest that the placement of a restoration decreases the stress compared to if the access were left open or temporized. The exception to this was found in the V-Taper group in which the sample with no restoration had a lower maximum stress than that of the V-Taper sample filled with resin. This is an irregularity in the results and may be attributed to higher stress concentrations that are found at the junction of two materials. Previous studies utilizing FEA have shown that in the preparation of canals, sharp points or edges can act as areas of stress concentration (39). This principle can be applied to the interface of the canal and pulp chamber providing a smooth transition to minimize points of localized stress.

The results of this study suggest that mandibular molars prepared with ProTaper Gold are more susceptible to fracture than those prepared with V-Taper 2H. In all samples, the maximum stress values were highest in the clinical crown with the greatest stress present at the CEJ. The results of this study are supported by Sabeti et al. who found that increasing the taper of the root canal preparation can reduce fracture resistance (67). Excessive instrument taper or root canal preparation taper may result in excessive removal of dentin and weakening of the root (68). The results of this study support the idea of a minimally tapered root canal preparation that has previously been described in literature (5,67,69–71).

Structural failure or fracture occurs when stresses exceed the ultimate strength of a material (72). The site of maximum tensile stress in the FEA model can be identified as the location in which a crack is most likely to begin. Sathorn used FEA to analyze the stress distribution of different canal preparations in a mandibular incisor and described that the crack propagation would be perpendicular to the surface in the location of maximum stress (39). Lam et al. assessed fracture loads in mandibular molars and found that incomplete fractures on the buccal surface were the most common fracture lines present in the study (37). Rundquist investigated the influence of root canal taper on root stresses and concluded that root fracture originating in the apical third is likely initiated during filling, while fracture originating in the cervical portion is likely caused by occlusal loads (38). Modern instrumentation and obturation techniques have reduced the historical risk of fracture occurring during obturation.

There is a debate as to where vertical root fractures originate with some researchers believing that they begin at the apex and propagate coronally, while others believe that they occur in the middle part of the root (73–75). Modern obturation techniques as continuous wave or single cone with bioceramic sealer do not predispose the apical root structure to the high apical forces that are needed with cold lateral compaction. Therefore, the focus should should be on the coronal and middle third where there is the most variation during the instrumentation process. The stress values in this analysis decreased apically through the root. The results of this study align with the findings of multiple studies that show the highest stresses are found in the coronal and middle thirds of the root (38,76).

Total deformation has not been used extensively in in dental FEA. Total deformation is the vector sum of all directional displacements of the body which is commonly described as strain. The goal of a dental restoration is to minimize or control deformation of surrounding tooth structure (77). The results of this study showed that models without the resin filling had higher deformation values than those with the resin filling. The delay of crown placement after root canal treatment has been found to significantly affect the survival rate of endodontically treated teeth (78). This study supports immediate or prompt restoration of endodontically treated teeth without a cotton pellet or sponge in order to reduce the risk of failure and fracture.

FEA can provide detailed quantitative and qualitative data any where within the mathematical model, but assumptions are made when the model is created. The assumptions made in this study were that the materials were linearly elastic and isotropic which is a common assumption in dental FEA (79). A singular static load was applied in this study in a simulated Class I occlusion scheme. This application of load was used to determine the most likely occlusion scenario, but it is limited to only providing that data and no excursive movements. This static loading protocol is used as an initial step in the assessment of stress distribution within a sample. Aside from the limitations of the FEA, the plastic tooth model chosen for the study did not have separate enamel and dentin layers, so the entire clinical crown was made of dentin. This situation could be applicable in a crown prepped tooth that doesn't have full coverage, but it is not representative of a true situation. Additionally, the simulated teeth were not crowned. This study sought to compare the two instrument types, and each sample was identical allowing for a direct comparison.

While there are limitations due to the plastic tooth and lack of full coverage restorations, this was the only reliable method to compare two identical teeth prepared by different file systems. A prior finite element analysis study has digitally manipulated canal systems in order to generate different canal profiles, but this was a case of an incisor with a straight canal (39). Fracture resistant studies often show contradicting results due to variations in the number of samples, tooth types, inclusion criteria, and testing parameters (80). Krikeli et al. discussed the importance of standardized methods when completing *in vitro* studies and in the interpretation of the results (70). Recent publications support the use of 3-dimensionally printed teeth to provide a high level of standardization for the comparative evaluation of samples (81,82). There will always be limitations in FEA and *in vitro* studies, but innovative production and scanning methods will continue to improve to best replicate clinical protocols. Future studies are needed using improved FEA and clinical models to more accurately predict the biomechanical responses of endodontically treated teeth prepared by different file systems.

The concept of minimally invasive endodontic access and instrumentation is at the forefront of clinical debates among practitioners. Loss of tooth structure is one of the most important causes of fractures in endodontically treated teeth. While the mechanism of vertical root fracture is debated and not well defined, knowledge of contributing factors is an important treatment consideration. The results of this study and of other studies support use of minimally tapered instruments to facilitate the conservation of pericervical dentin and prevent unnecessary reduction in fracture resistance (5,31,67).

CONCLUSION

Within the limitations of this study, it can be concluded that the maximum stress values within the tooth prepared by ProTaper Gold were higher than those in the tooth prepared by V-Taper 2H. The minimally invasive instrumentation of the V-Taper 2H system preserves more pericervical dentin which may increase the resistance to fracture.

BIBLIOGRAPHY

1. Schilder H. Cleaning and shaping the root canal. Dent Clin North Am 1974;18(2):269–96.

2. Stewart GG. The importance of chemomechanical preparation of the root canal. Oral Surgery, Oral Med Oral Pathol 1955.

3. Byström A, Sundqvist G. Bacteriologic evaluation of the efficacy of mechanical root canal instrumentation in endodontic therapy. Eur J Oral Sci 1981;89(4):321–8.

4. Gluskin AH, Peters CI, Peters OA. Minimally invasive endodontics: Challenging prevailing paradigms. Br Dent J 2014.

5. Clark D, Khademi J. Modern Molar Endodontic Access and Directed Dentin Conservation. Dent Clin North Am 2010:249–73.

6. Byström A, Happonen R -P, Sjögren U, et al. Healing of periapical lesions of pulpless teeth after endodontic treatment with controlled asepsis. Dent Traumatol 1987.

7. Kakehashi S, Stanley HR, Fitzgerald RJ. The effects of surgical exposures of dental pulps in germ-free and conventional laboratory rats. Oral Surgery, Oral Med Oral Pathol 1965.

8. Möller ÅJR, Fabricius L, Dahlén G, et al. Apical periodontitis development and bacterial response to endodontic treatment. Experimental root canal infections in monkeys with selected bacterial strains. Eur J Oral Sci 2004.

9. Ricucci D, Siqueira JF. Biofilms and apical periodontitis: Study of prevalence and association with clinical and histopathologic findings. J Endod 2010.

10. Hulsmann M, Peters OA, Dummer PMH. Mechanical preparation of root canals: shaping goals, techniques and means. Endod Top 2005.

11. Nair PNR, Sjögren U, Krey G, et al. Intraradicular bacteria and fungi in root-filled, asymptomatic human teeth with therapy-resistant periapical lesions: A long-term light and electron microscopic follow-up study. J Endod 1990.

12. Wu MK, R'oris A, Barkis D, et al. Prevalence and extent of long oval canals in the apical third. Oral Surg Oral Med Oral Pathol Oral Radiol Endod 2000.

13. Kerekes K, Tronstad L. Morphometric observations on the root canals of human molars. J Endod 1977.

14. Kuttler Y. Microscopic investigation of root apexes. J Am Dent Assoc 1955.

15. Spångberg L. The wonderful world of rotary root canal preparation. Oral Surg Oral Med Oral Pathol Oral Radiol Endod 2001.

16. Yared GM, Bou Dagher FE. Influence of apical enlargement on bacterial infection during treatment of apical periodontitis. J Endod 1994.

17. Ørstavik D, Qvist V, Stoltze K. A multivariate analysis of the outcome of endodontic treatment. Eur J Oral Sci 2004.

18. Siqueira JF. Histological evaluation of the effectiveness of five instrumentation techniques for cleaning the apical third of root canals. J Endod 1997.

19. Peters OA, Peters CI, Basrani B. Cleaning and Shaping the Root Canal System. In: Hargreaves KM Berman LH, editor. *Cohen's Pathways Pulp*. 11th ed. St. Louis: Elsevier; 2016. p. 226.

20. Young GR, Parashos P, Messer HH. The principles of techniques for cleaning root canals. Aust Dent J 2007.

21. Arias A, Singh R, Peters OA. Torque and force induced by ProTaper universal and ProTaper next during shaping of large and small root canals in extracted teeth. J Endod 2014.

22. Clauder T, Baumann MA. ProTaper NT system. Dent Clin North Am 2004.

23. Ruddle CJ. the Protaper Advantage: Shaping the Future of Endodontics. Dent Today 2001.

24. Chang SW, Shim KS, Kim YC, et al. Cyclic fatigue resistance, torsional resistance, and metallurgical characteristics of V taper 2 and V taper 2H rotary NiTi files. Scanning 2016.

25. Clark D, Khademi J, Herbranson E. Fracture resistant endodontic and restorative preparations. Dent Today 2013.

26. Ericson D. What is minimally invasive dentistry? Oral Health Prev Dent 2004;2 Suppl 1:287–92.

27. Christie WH, Thompson GK. The importance of endodontic access in locating maxillary and mandibular molar canals. J Can Dent Assoc 1994.

28. Goerig AC, Michelich RJ, Schultz HH. Instrumentation of root canals in molar using the step-down technique. J Endod 1982.

29. Clark D, Khademi JA. Case Studies in Modern Molar Endodontic Access and Directed Dentin Conservation. Dent Clin North Am 2010.

30. Allen C, Meyer C, Yoo E, et al. Stress distribution in a tooth treated through minimally invasive access compared to one treated through traditional access: A finite element analysis study. J Conserv Dent 2018.

31. Zhang Y, Liu Y, She Y, et al. The Effect of Endodontic Access Cavities on Fracture Resistance of First Maxillary Molar Using the Extended Finite Element Method. J Endod 2019.

32. Özyürek T, Ülker Ö, Demiryürek EÖ, et al. The Effects of Endodontic Access Cavity Preparation Design on the Fracture Strength of Endodontically Treated Teeth: Traditional Versus Conservative Preparation. J Endod 2018.

33. Jiang Q, Huang Y, Tu XR, et al. Biomechanical Properties of First Maxillary Molars with Different Endodontic Cavities: A Finite Element Analysis. J Endod 2018;44(8):1283–8.

34. Bender IB, Freedland JB. Adult root fracture. J Am Dent Assoc 1983.

35. Dammaschke T, Eleazer, PD; Glickman, GN; McClanahan, SB; Webb, TD; Justman B. *Glossary of Endodontic Terms*. 2015.

36. Wilcox LR. The relationship of root canal enlargement to finger-spreader induced vertical root fracture. J Endod 1997.

37. Lam PPS, Palamara JEA, Messer HH. Fracture strength of tooth roots following canal preparation by hand and rotary instrumentation. J Endod 2005.

38. Rundquist BD, Versluis A. How does canal taper affect root stresses? Int Endod J 2006.

39. Sathorn C, Palamara JEA, Palamara D, et al. Effect of root canal size and external root surface morphology on fracture susceptibility and pattern: A finite element analysis. J Endod 2005.

40. Fonzar F, Fonzar A, Buttolo P, et al. The prognosis of root canal therapy: a 10-year retrospective cohort study on 411 patients with 1175 endodontically treated teeth. Eur J Oral Implantol 2009.

41. Shon W-J. Introducing the GentleWave System. Restor Dent Endod 2016.

42. Knowles NC. Finite element analysis. Comput Des 1984.

43. van Staden RC, Guan H, Loo YC. Application of the finite element method in

dental implant research. Comput Methods Biomech Biomed Engin 2006.

44. Rubin C, Krishnamurthy N, Capilouto E, et al. Clinical Science: Stress Analysis of the Human Tooth Using a Three-dimensional Finite Element Model. J Dent Res 1983.

45. Ho MH, Lee S yuan, Chen HH, et al. Three-dimensional finite element analysis of the effects of posts on stress distribution in dentin. J Prosthet Dent 1994.

46. Ko C-C. Past, Present and Future of Finite Element Analysis in Dentistry. In: Moratal David, editor. *Finite Elem. Anal. - From Biomed. Appl. to Ind. Dev.* InTech; 2012. p. 3–24.

47. Trivedi S. Finite element analysis: A boon to dentistry. J Oral Biol Craniofacial Res 2014.

48. Gao J, Xu W, Ding Z. 3D finite element mesh generation of complicated tooth model based on CT slices. Comput Methods Programs Biomed 2006;82(2):97–105.

49. Zannoni C, Mantovani R, Viceconti M. Material properties assignment to finite element models of bone structures: A new method. Med Eng Phys 1999.

50. Abdulmunem M, Dabbagh A, Naderi S, et al. Evaluation of the effect of dental cements on fracture resistance and fracture mode of teeth restored with various dental posts: A finite element analysis. J Eur Ceram Soc 2016.

51. Alikhasi M, Siadat H, Geramy A, et al. Stress distribution around maxillary anterior implants as a factor of labial bone thickness and occlusal load angles: A 3-dimensional finite element analysis. J Oral Implantol 2014.

52. Adanir N, Belli S. Stress Analysis of a Maxillary Central Incisor Restored with Different Posts. Eur J Dent 2007.

53. Yan X, Zhang X, Gao J, et al. Maxillary Sinus Augmentation without Grafting Material with Simultaneous Implant Installation: A Three-Dimensional Finite Element Analysis. Clin Implant Dent Relat Res 2015.

54. Hsu M-L, Chen F-C, Kao H-C, et al. Influence of off-axis loading upon an anterior maxillary implant: a 3-dimensional finite element analysis. J Biomech 2006.

55. Kim KY, Bayome M, Park JH, et al. Displacement and stress distribution of the maxillofacial complex during maxillary protraction with buccal versus palatal plates: Finite element analysis. Eur J Orthod 2015.

56. Durmuş G, Oyar P. Effects of post core materials on stress distribution in the

restoration of mandibular second premolars: A finite element analysis. J Prosthet Dent 2014.

57. Liang R, Guo W, Qiao X, et al. Biomechanical analysis and comparison of 12 dental implant systems using 3D finite element study. Comput Methods Biomech Biomed Engin 2015.

58. Huysmans M, Peters M, Varst P, et al. Failure behaviour of fatigue-tested post and cores. Int Endod J 1993.

59. Tamse A, Fuss Z, Lustig J, et al. An evaluation of endodontically treated vertically fractured teeth. J Endod 1999.

60. Cohen S, Blanco L, Berman L. Vertical root fractures: Clinical and radiographic diagnosis. J Am Dent Assoc 2003.

61. Abou-Rass M, Frank AL, Glick DH. The anticurvature filing method to prepare the curved root canal. J Am Dent Assoc 1980.

62. Allen C, Meyer C, Yoo E, et al. Stress distribution in a tooth treated through minimally invasive access compared to one treated through traditional access: A finite element analysis study. J Conserv Dent 2018.

63. Krishan R, Paqué F, Ossareh A, et al. Impacts of conservative endodontic cavity on root canal instrumentation efficacy and resistance to fracture assessed in incisors, premolars, and molars. J Endod 2014.

64. Plotino G, Grande NM, Isufi A, et al. Fracture Strength of Endodontically Treated Teeth with Different Access Cavity Designs. J Endod 2017.

65. Jiang Q, Huang Y, Tu XR, et al. Biomechanical Properties of First Maxillary Molars with Different Endodontic Cavities: A Finite Element Analysis. J Endod 2018.

66. Silva EJNL, Rover G, Belladonna FG, et al. Impact of contracted endodontic cavities on fracture resistance of endodontically treated teeth: a systematic review of in vitro studies. Clin Oral Investig 2018.

67. Sabeti M, Kazem M, Dianat O, et al. Impact of Access Cavity Design and Root Canal Taper on Fracture Resistance of Endodontically Treated Teeth: An Ex Vivo Investigation. J Endod 2018.

68. Pilo R. Residual dentin thickness in mandibular premolars prepared with hand and rotatory instruments. J Endod 1998.

69. Zandbiglari T, Davids H, Schäfer E. Influence of instrument taper on the resistance

to fracture of endodontically treated roots. Oral Surg Oral Med Oral Pathol Oral Radiol Endod 2006.

70. Krikeli E, Mikrogeorgis G, Lyroudia K. In Vitro Comparative Study of the Influence of Instrument Taper on the Fracture Resistance of Endodontically Treated Teeth: An Integrative Approach–based Analysis. J Endod 2018;44(9):1407–11.

71. Singla M, Aggarwal V, Logani A, et al. Comparative evaluation of rotary ProTaper, Profile, and conventional stepback technique on reduction in Enterococcus faecalis colony-forming units and vertical root fracture resistance of root canals. Oral Surgery, Oral Med Oral Pathol Oral Radiol Endodontology 2010.

72. Callister WD. Materials science and engineering: An introduction (2nd edition). Mater Des 1991.

73. Saw LH, Messer HH. Root strains associated with different obturation techniques. J Endod 1995.

74. Harvey TE, White JT, Leeb IJ. Lateral condensation stress in root canals. J Endod 1981.

75. Dang DA, Walton RE. Vertical root fracture and root distortion: Effect of spreader design. J Endod 1989.

76. Ricks-Williamson LJ, Fotos PG, Goel VK, et al. A three-dimensional finite-element stress analysis of an endodontically prepared maxillary central incisor. J Endod 1995.

77. Costa AKF, Xavier TA, Paes-Junior TJA, et al. Influence of occlusal contact area on cusp deflection and stress distribution. J Contemp Dent Pract 2015.

78. Pratt I, Aminoshariae A, Montagnese TA, et al. Eight-Year Retrospective Study of the Critical Time Lapse between Root Canal Completion and Crown Placement: Its Influence on the Survival of Endodontically Treated Teeth. J Endod 2016.

79. Hsu M-L, Chang C-L. Application of Finite Element Analysis in Dentistry. *Finite Elem. Anal.* 2010.

80. Abou-Elnaga MY, Alkhawas MBAM, Kim HC, et al. Effect of Truss Access and Artificial Truss Restoration on the Fracture Resistance of Endodontically Treated Mandibular First Molars. J Endod 2019;45(6):813–7.

81. Connert T, Krug R, Eggmann F, et al. Guided Endodontics versus Conventional Access Cavity Preparation: A Comparative Study on Substance Loss Using 3-dimensional–printed Teeth. J Endod 2019.

82. Gok T, Capar ID, Akcay I, et al. Evaluation of Different Techniques for Filling Simulated C-shaped Canals of 3-dimensional Printed Resin Teeth. J Endod 2017.